Suppression of Microtubule Dynamic Instability by the +TIP Protein EB1 and Its Modulation by the CAP-Gly Domain of p150^{Glued}†

Tapas Manna,‡ Srinivas Honnappa,§ Michel O. Steinmetz,§ and Leslie Wilson*,‡

Department of Molecular, Cellular, and Developmental Biology and the Neuroscience Research Institute, University of California Santa Barbara, Santa Barbara, California 93106, and Biomolecular Research, Structural Biology, Paul Scherrer Institut, Villigen PSI, Switzerland

Received September 19, 2007; Revised Manuscript Received November 7, 2007

ABSTRACT: The EB1+TIP protein family and its binding partners track growing plus ends of microtubules in cells and are thought to regulate their dynamics. Here we determined the effects of EB1 and the N-terminal CAP-Gly domain (p150n) of one of its major binding partners, p150^{Glued}, both separately and together, on the dynamic instability parameters at plus ends of purified steady-state microtubules. With EB1 alone, the shortening rate, the extent of shortening, and the catastrophe frequency were suppressed in the absence of significant effects on the growth rate or rescue frequency. The effects of EB1 on dynamics were significantly different when p150n was added together with EB1. The rate and extent of shortening and the catastrophe frequency were suppressed 3−4 times more strongly than with EB1 alone. In addition, the EB1−p150n complex increased the rescue frequency and the mean length the microtubules grew, parameters that were not significantly affected by EB1 alone. Similarly, deletion of EB1's C-terminal tail, which is a crucial binding region for p150n, significantly increased the ability of EB1 to suppress shortening dynamics. EB1 by itself bound along the length of the microtubules with 1 mol of EB1 dimer bound per ∼12 mol of tubulin dimer. Approximately twice the amount of EB1 was recruited to the microtubules in the presence of p150n. Our results indicate that inactivation of EB1's flexible C-terminal tail significantly changes EB1's ability to modulate microtubule dynamics. They further suggest that p150^{Glued} may activate and thereby facilitate the recruitment of EB1 to the tips of microtubules to regulate their dynamics.

The stochastic switching between growth and shortening (dynamic instability) at the plus ends of microtubules plays important roles in cell migration, motility and mitosis (*1*−*3*). Microtubule associated or accessory proteins (MAPs[1]) are known to regulate dynamic instability behaviors, both *in vitro* and in cells (*4*, *5*). The plus end tracking proteins (+TIPs) are MAPs that localize to and track the plus ends of growing microtubules in cells (*6*−*19*). +TIPs, which include EB1 (end binding protein 1), the p150^{Glued} subunit of dynactin, CLIP170 (cytoplasmic linker protein 170) and APC (adenomatous polyposis coli protein), are strongly conserved and found in species from yeast to humans. A number of functions have been attributed to the +TIPs including involvement in the search and capture dynamics of microtubule plus ends in relation to targeting chromosomes during mitosis and targeting to the cell cortex during interphase. Several of the +TIP proteins including EB1, p150^{Glued}, CLIP170, and APC have been shown to bind to each other *in vitro* and to colocalize at growing microtubule plus ends in cells (*7*−*13*). Their interactions are of moderate affinities and rely on a limited set of protein modules and linear sequence motifs (*20*−*23*). This finding suggests that numerous modular binding sites in different combinations control the dynamics and remodeling of +TIP networks.

Evidence is accumulating that EB1 and its binding partners regulate microtubule plus end growth, stability, and dynamics. When EB1 is added to *Xenopus* egg extracts, it binds to the microtubules both at their ends and along their lengths (*14*). In this system, the added EB1 was found to suppress the catastrophe frequency (the switching frequency from growth to rapid shortening), to increase the rescue frequency (the switching frequency from shortening to growth) and to suppress the rate of shortening, leading to its description as an anticatastrophe factor (*14*). However, it is not clear from these studies how EB1 is acting at a mechanistic level because it was present together with endogenous EB1 and +TIP binding partners.

There are no data available describing how EB1 regulates the dynamics of purified microtubules either alone or in combination with other +TIP proteins. One of the important +TIP binding partners of EB1 is p150^{Glued}, a subunit of dynactin which is a major component of the dynein−dynactin

† This study was supported by USPHS Grant NS13560, by U.S. National Science Foundation Grant 0331697, and by the Swiss National Science Foundation through Grant 3100A0-109423 (to M.O.S.).

* Author to whom correspondence should be sent. E-mail: wilson@lifesci.ucsb.edu. Fax: 805-893-8094. Tel: 805-893-2819.

‡ University of California Santa Barbara.

§ Paul Scherrer Institut.

[1] Abbreviations: EB1, end-binding protein 1; +TIP(s), microtubule plus end tracking protein(s); APC, adenomatous polyposis coli protein; CLIP170 (cytoplasmic linker protein 170); MAP(s), microtubule-associated/accessory protein(s); CAP-Gly, cytoskeleton associated protein-glycine rich; PMME buffer, 87 mM Pipes, 36 mM Mes, 1.4 mM $MgCl_2$, 1 mM EGTA, pH 6.8.

10.1021/bi701912g CCC: $40.75
Published on Web 12/15/2007

motor complex (*15*). p150^{Glued} localizes at the plus ends of growing microtubules along with other +TIPs including EB1 and CLIP170 (*16*). p150^{Glued} has been shown to bind directly to EB1 and to microtubules (*17*, *18*) and in cells appears to be involved in dynein-mediated transport of cargo along microtubules and required for the maintenance of radial microtubule arrays (*19*).

p150^{Glued} binds to the EB1-like domain and to the flexible C-terminal tail (20 amino acids) of EB1 through its N-terminal CAP-Gly (cytoskeletal associated protein-glycine rich) domain (*20*). The N-terminal CAP-Gly domain of p150^{Glued} (called p150n) forms a complex with EB1 of moderate stability consisting of two molecules of p150n and one molecule of EB1 dimer (*20*, *21*, *23*). The CAP-Gly domain itself also binds to microtubules although not very efficiently (*18*). It has also been shown to increase EB1's ability to induce microtubule assembly *in vitro* and is thought to trigger EB1 to an activated conformation (*21*). However, it is not known how such activation might modulate EB1's ability to regulate microtubule dynamics.

In the present study we determined the effects of EB1 on dynamic instability at plus ends of purified microtubules at steady state in the absence and presence of p150n. We found that EB1 by itself stabilized plus ends by suppressing shortening dynamics without significantly affecting growth dynamics. Interestingly, the potency of EB1 was increased 3−4-fold when bound to p150n. In addition to its strong ability to suppress plus end shortening, the EB1−p150n complex, in contrast with EB1 alone, increased the length microtubules grew during growth events and increased the rescue frequency. Deletion of EB1's C-terminal tail (fragment denoted EB1-ΔC), which is the major binding site for p150n, significantly increased the ability of EB1 to suppress dynamics, making it as efficient as the full length EB1−p150n complex. Together with results of experiments showing that EB1 and EB1−p150n bind to microtubules, the results indicate that EB1 by itself suppresses plus end shortening dynamics by binding along the surface of microtubules and that p150n activates EB1 to modulate both shortening and growth dynamics, possibly by acting in addition as a complex directly at the plus ends.

MATERIALS AND METHODS

Tubulin, EB1, EB1-ΔC and p150n Constructs and Proteins. Cloning of full length human EB1 into a modified pET-15b vector (Novagen) has been described previously (*22*). For the EB1-ΔC fragment (residues 1−248), the EB1 cDNA was used as a template for PCR amplification. The PCR product was ligated into the same modified pET-15b as the full length construct. The cDNA of the p150^{Glued} CAP-Gly domain (p150n, residues 18−111) was subcloned into pET-15b at the *Nde*I and *Bam*HI sites. Proteins were expressed in bacterial strain BL21 (DE3) and purified on HiTrap Ni^{2+}-Sepharose chelating columns (Amersham Bioscience, U.K.) as described (*20*, *22*). After cleavage of the 6x His-tag at 4 °C overnight with thrombin, the proteins were subjected to gel filtration on a Superdex-75 column (Amersham) equilibrated in 10 mM Tris, pH 7.5, supplemented with 50 mM NaCl. The proteins were finally dialyzed against 50 mM Pipes buffer, pH 6.8. Highly purified bovine brain tubulin was prepared as described previously (*24*). Protein concentrations throughout this work were determined by the method of Bradford with bovine serum albumin as the standard (*25*).

Video Microscopy. Purified tubulin (20 μM) was assembled onto the ends of sea urchin (*Strongylocentrotus purpuratus*) axoneme seeds in PMME buffer plus 2 mM GTP at 30 °C in the presence or absence of EB1, EB1-ΔC or p150n, and incubated at 30 °C for 40 min to achieve steady state (confirmed by light scattering at 350 nm). The concentrations of EB1, EB1-ΔC and p150n used in these experiments had negligible effects on the steady-state polymer concentration (data not shown). Analysis of dynamic instability at plus ends was carried out at 30 °C by video-enhanced differential interference contrast microscopy as previously described (*26*). Briefly, the plus ends were identified and distinguished from minus ends on the basis of their fast growth rates, the number of microtubules that grew at the ends, and the relative lengths of the microtubules. The growth rates, shortening rates, and transition frequencies were determined as previously described (*26*). We considered microtubules to be growing if they increased in length >0.3 μm at a rate >0.3 μm/min. Shortening events were identified by a >1 μm length change at a rate of >2 μm/min. Microtubules that changed <0.3 μm/min over a duration of 4 data points were considered to be in an attenuated state. Between 25 and 40 microtubules were analyzed for each condition.

EB1, EB1-ΔC and EB1−p150n Binding to Microtubules. For quantitation of full length EB1 or EB1-ΔC binding to microtubules, tubulin (20 μM) and EB1 proteins (3.4 μM EB1 dimer concentration) or mixture of EB1 and p150n (6.8 μM as monomers for each) were assembled with glycerol-stabilized sheared nucleating microtubule seeds in PMME buffer (10% vol/vol) for 40 min at 37 °C (*27*). The microtubules were then sedimented through a 30% sucrose cushion and the pellets resuspended in PMME buffer and subjected to SDS−PAGE followed by Coomassie Blue staining. The amounts of full length EB1 or EB1-ΔC bound to microtubules were determined by densitometric analysis of the gel bands as described previously (*27*). The amount of tubulin in each pellet was determined by subtracting the amount of EB1 protein present from the total amount of protein (tubulin and EB1) loaded onto the gel lane.

RESULTS

EB1 Suppresses Dynamic Instability at Plus Ends of Steady-State Microtubules in Vitro. We first wanted to determine how EB1 by itself modulates dynamic instability at plus ends of purified microtubules at steady state, conditions at which the microtubule polymer mass and soluble tubulin concentrations remain constant and a direct action of EB1 on microtubules independent of any possible effects due to changes in the soluble tubulin concentration can be determined (*26*). Solutions of purified tubulin (20 μM) were polymerized to steady state (30 °C, 40 min) in the presence of different concentrations of EB1, and the dynamics parameters at plus ends of individual microtubules were analyzed. As shown in Figure 1A and Table 1, 1 μM EB1, equivalent to a 1:40 molar ratio of EB1 dimer to tubulin (1 μM EB1 monomer = 0.5 μM EB1 dimer), reduced the shortening rate by ∼35% from 27.6 ± 4.3 to 18.1 ± 3.6 μm per min and the length shortened by ∼30% from 7.2 ± 0.5

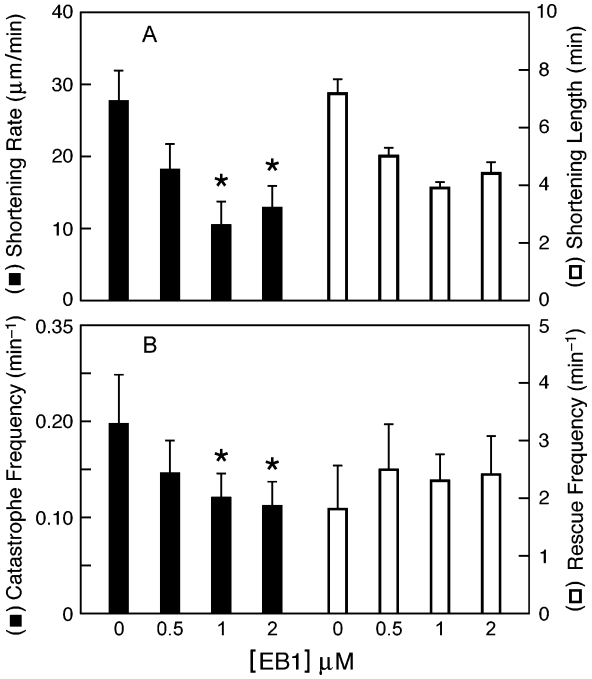

FIGURE 1: Effects of EB1 alone on plus end dynamic instability parameters at steady state *in vitro*. A. Effects on the shortening rate (solid bars) and the length shortened during individual shortening events (unshaded bars). B. Effect of EB1 alone on the catastrophe frequency (solid bars) and the rescue frequency (unshaded bars). Error bars for the shortening rate and the catastrophe and rescue frequencies are SD. The error bars on the shortening lengths are SEM. (*) $P = 0.001$. Tubulin concentration was 20 μM.

to 5.0 ± 0.3 μm. At a 1:20 molar ratio of EB1 dimer to tubulin in the system, the rate and extent of shortening were further reduced (~70% and ~40%, respectively). No further reduction occurred by increasing the EB1 dimer to tubulin ratio to 1:10. EB1 moderately reduced the catastrophe frequency (the frequency of switching from growth to shortening) (Figure 1B, Table 1). The catastrophe frequency was reduced by 30% at an EB1 dimer to tubulin ratio of 1:40 and was reduced maximally by 40% at a ratio of 1:20. EB1 did not significantly affect the rescue frequency (Figure 1B, Table 1). Surprisingly, EB1 alone did not exert any significant effect on the growth rate or the length the microtubules grew during a growth event (Table 1). The combined effects on the individual parameters resulted in an increase in the fraction of time the microtubules remained in an attenuated state, neither growing nor shortening detectably, and a decrease of the overall dynamicity (Table 1).

p150n Increases EB1's Ability To Suppress Shortening Dynamics and Modifies Its Ability To Regulate Growth Dynamics. One of the binding partners believed to act together with EB1 at microtubule plus ends is $p150^{Glued}$ (*28*). There are two identical binding sites for the CAP-Gly domain of $p150^{Glued}$ (p150n) per EB1 dimer (K_d, ~2 μM) (*20*, *23*). Thus, we wanted to determine whether p150n modulates the effects of EB1 on dynamic instability. We first analyzed the effects of the p150n monomer itself. In contrast to EB1 alone, molar ratios of p150n to tubulin of 1:30 and 1:10 did not appreciably change the rate or extent of shortening or the catastrophe frequency (Table 2). However, in contrast with EB1, p150n significantly increased the length the microtubules grew during growth events although it did so only at high concentrations. Specifically, a molar ratio of p150n:tubulin of 1:10 increased the growth length ~1.5-fold. Also unlike EB1, p150n significantly increased the rescue frequency (a 1:10 molar ratio of p150n monomer:tubulin increased the rescue frequency by ~40%) (Tables 1, 2). Consistent with its effects on these parameters at high concentrations, p150n significantly increased the fraction of time the microtubules grew.

In order to determine how p150n might affect the ability of EB1 to modulate dynamics, tubulin was polymerized to steady state in the presence of various concentrations of EB1−p150n mixtures that were prepared by incubating solutions of the two proteins for 20 min at room temperature in PMME buffer at a ratio of 2 mol of p150n monomer to 1 mol of EB1 dimer. As shown in Figure 2A and Table 3, the EB1−p150n mixture suppressed the rate and extent of shortening significantly more strongly than EB1 alone. The mixture of 0.17 μM EB1 dimer and 0.34 μM p150n (only a 1:120 ratio of EB1 dimers to tubulin) reduced both the shortening rate and the length shortened during individual shortening events by ~30%. A maximal suppression of the rate (~60%) and extent (~50%) of shortening occurred at a ~1:80 molar ratio of EB1−p150n to tubulin. This same suppression of shortening by EB1 alone required ~4-fold higher concentration of EB1 (compare Tables 1 and 3).

While p150n by itself did not appreciably reduce the catastrophe frequency (Table 2), EB1−p150n strongly suppressed this parameter (Figure 2B, Table 3) and did so 3−4-

Table 1: Effects of EB1 on Dynamic Instability at Microtubule Plus Ends[a]

	EB:tubulin			
	control (0)	1:40	1:20	1:10
growth rate (μm/min)	1.34 ± 0.3 (41)	1.4 ± 0.6 (44)	1.4 ± 0.6 (38)	1.52 ± 0.4 (40)
growth length (μm)	2.2 ± 0.3	2.0 ± 0.2	1.9 ± 0.2	2.7 ± 0.3
shortening rate (μm/min)	27.6 ± 4.3 (33)	18.1 ± 3.6 (35)	10.44 ± 3.3* (33)	12.8 ± 3.1* (32)
shortening length (μm)	7.2 ± 0.5	5.0 ± 0.3	3.9 ± 0.2	4.4 ± 0.2
catastrophe frequency (events/min)	0.23 ± 0.06 (33)	0.16 ± 0.04 (35)	0.14 ± 0.03* (33)	0.13 ± 0.03* (32)
rescue frequency (events/min)	1.8 ± 0.8 (26)	2.5 ± 0.9 (30)	2.3 ± 0.5 (25)	2.4 ± 0.7 (27)
percentage of time				
growing	58.6	51.6	42.6	46.4
shortening	5.6	4.4	4.3	4.4
attenuated	35.8	44.0	58.1	49.2
dynamicity (μm/min)	2.35	1.5	1.0	1.2

[a] [Tubulin] = 20 μM. [EB1] refers to the dimer. Data are mean ± SD. *$P = 0.001$ except for growing and shortening lengths, which are mean ± SEM. Values in the parentheses are the number of events.

Table 2: Effect of p150n on Dynamic Instability at Microtubule Plus Ends[a]

	p150n:tubulin		
	control (0)	1:30	1:10
growth rate (μm/min)	1.34 ± 0.3 (41)	1.45 ± 0.6 (13)	1.6 ± 0.6 (45)
growth length (μm)	2.2 ± 0.3	2.8 ± 0.8	3.9 ± 0.5*
shortening rate (μm/min)	27.6 ± 4.3 (33)	29.7 ± 7.4 (11)	24.9 ± 4.9 (38)
shortening length (μm)	7.2 ± 0.5	7.4 ± 0.8	6.4 ± 0.3
catastrophe frequency (events/min)	0.23 ± 0.06 (33)	0.26 ± 0.05 (11)	0.2 ± 0.05 (38)
rescue frequency (events/min)	1.8 ± 0.8 (26)	2.3 ± 0.9 (11)	3.0 ± 0.7** (37)
percentage of time			
growing	58.6	64.8	74.8
shortening	5.6	5.6	5.0
attenuated	35.8	29.6	20.2
dynamicity (μm/min)	2.35	2.5	2.3

[a] [Tubulin] = 20 μM, * $P = 0.001$. ** $P = 0.01$. Data are mean ± SD, except for growing and shortening lengths, which are mean ± SEM. Values in the parentheses are the number of events. Control data are the same as those shown in Table 1, reproduced here for the convenience of the reader.

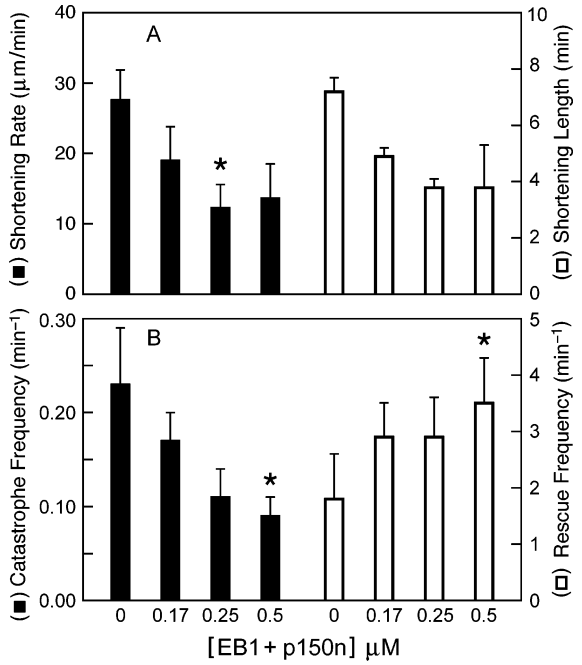

FIGURE 2: Effects of the EB1−p150n mixture on plus end dynamic instability parameters at steady state. A. Effects on the shortening rate (solid bars) and the length shortened during individual shortening events (unshaded bars). B. Effect on the catastrophe frequency (solid bars) and the rescue frequency (unshaded bars). Error bars for the shortening rate and the catastrophe and rescue frequencies are SD. The error bars for the shortening lengths are SEM. (*) $P = 0.0001$. Tubulin concentration was 20 μM.

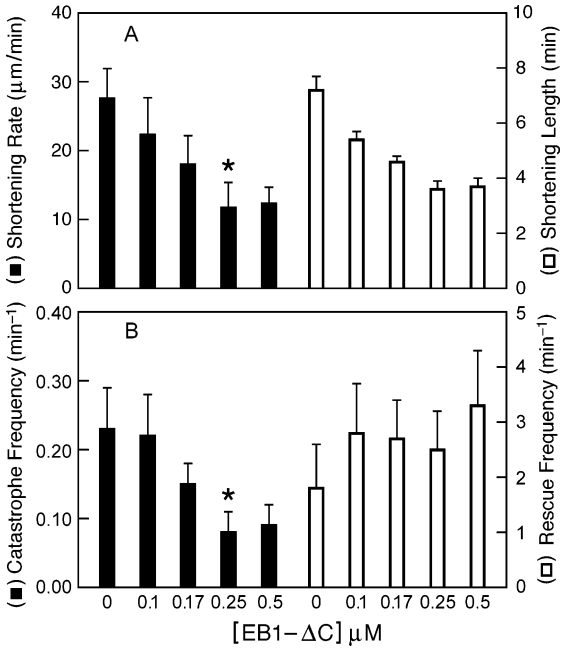

FIGURE 3: Effect of EB1-ΔC on plus end dynamic instability parameters at steady state. A. Effect of EB1-ΔC on the shortening rate (solid bars) and the length shortened during individual shortening events (unshaded bars). B. Effect of EB1-ΔC on the catastrophe frequency (solid bars) and the rescue frequency (unshaded bars) at plus ends. Error bars for the shortening rate and the catastrophe and rescue frequencies are SD. The error bars for the shortening lengths are SEM. (*) $P = 0.0001$. Tubulin concentration was 20 μM.

fold more strongly than EB1 itself. For example, only a 1:120 molar ratio of EB1−p150n to tubulin decreased the catastrophe frequency by 30%, and a 1:40 molar ratio of EB1−p150n:tubulin reduced this parameter by ~60% (Table 3). A similar extent in reduction of this parameter by EB1 itself required 3−4-fold higher concentration of EB1 (compare Figures 1B and 2B). In contrast to the lack of effect of EB1 by itself on the rescue frequency, EB1−p150n significantly increased the rescue frequency (Figure 2B, Table 3). For example, only 0.25 μM EB1−p150n, corresponding to a 1:80 molar ratio of EB1−p150n to tubulin, increased the rescue frequency by ~1.7-fold. A similar extent of increase of the rescue frequency by p150n itself required ~4-fold higher concentration of p150n (compare Tables 2 and 3).

In addition, EB1−p150n increased the length the microtubules grew significantly more strongly than p150n by itself. Only a 1: 80 molar ratio of EB1−p150n:tubulin increased the growth length ~1.8-fold (Table 3). A similar increase in this parameter by p150n itself required a ~4-fold higher concentration of p150n (Table 2).

The C-Terminal Tail of EB1 Negatively Regulates the Ability of EB1 To Suppress Shortening Dynamics. Because the C-terminal 20 amino acids of EB1 are a crucial region for p150n binding (*20*, *21*, *23*), we wanted to determine if the region might regulate the ability of EB1 to suppress shortening dynamics. Based on circular dichroism and X-ray crystallographic analyses it was found that this C-terminal EB1 segment was disordered in solution (*22*). The plus end dynamic instability parameters in the absence and presence of C-terminally truncated EB1 alone (EB1-ΔC) are shown in Table 4. EB1-ΔC suppressed the rate and extent of

Table 3: Effect of EB1−p150n Complex on Dynamic Instability at Microtubule Plus Ends[a]

	EB1−p150n:tubulin			
	control (0)	1:120	1:80	1:40
growth rate (μm/min)	1.34 ± 0.3 (41)	1.5 ± 0.6 (49)	1.5 ± 0.7 (46)	1.6 ± 0.7 (42)
growth length (μm)	2.2 ± 0.3	3.4 ± 0.3	3.8 ± 0.3	4.6 ± 0.6*
shortening rate (μm/min)	27.6 ± 4.3 (33)	19.0 ± 4.8 (37)	12.3 ± 3.3* (34)	13.7 ± 4.8* (33)
shortening length (μm)	7.2 ± 0.5	4.9 ± 0.3	3.8 ± 0.3	3.8 ± 1.5
catastrophe frequency (events/min)	0.23 ± 0.06 (33)	0.17 ± 0.03 (37)	0.11 ± 0.03* (34)	0.09 ± 0.02* (33)
rescue frequency (events/min)	1.8 ± 0.8 (26)	2.9 ± 0.6 (34)	2.9 ± 0.7 (31)	3.5 ± 0.8 (32)
percentage of time				
growing	58.6	62.7	66.6	70.0
shortening	5.6	4.3	3.5	2.6
attenuated	35.8	33	29.9	27.4
dynamicity (μm/min)	2.35	1.6	1.3	1.3

[a] [Tubulin] = 20 μM, * $P = 0.001$. Data are mean ± SD except for growing and shortening lengths, which are mean ± SEM. The values in the parentheses are the number of events. Control data are the same as those shown in Table 1, reproduced here for the convenience of the reader.

Table 4: Effect of EB1-ΔC on Dynamic Instability at Microtubule Plus Ends[a]

	EB1-ΔC:tubulin				
	control (0)	1:200	1:120	1:80	1:40
growth rate (μm/min)	1.34 ± 0.3 (41)	1.5 ± 0.7 (48)	1.45 ± 0.6 (43)	1.5 ± 0.5 (36)	1.5 ± 0.6 (46)
growth length (μm)	2.2 ± 0.3	2.6 ± 0.4	2.7 ± 0.2	3.0 ± 0.3	2.9 ± 0.3
shortening rate (μm/min)	27.6 ± 4.3 (33)	22.3 ± 5.4 (34)	18.0 ± 4.2 (37)	11.5 ± 3.7* (32)	12.3 ± 2.4* (37)
shortening length (μm)	7.2 ± 0.5	5.4 ± 0.3	4.6 ± 0.2	3.6 ± 0.3	3.7 ± 0.3
catastrophe frequency (events/min)	0.23 ± 0.06 (33)	0.22 ± 0.06 (34)	0.15 ± 0.03 (37)	0.08 ± 0.02* (32)	0.10 ± 0.03* (37)
rescue frequency (events/min)	1.8 ± 0.8 (26)	2.8 ± 0.9 (30)	2.7 ± 0.7 (32)	2.5 ± 0.7 (29)	3.3 ± 1.0 (35)
percentage of time					
growing	58.6	58.1	51.6	43.4	52.7
shortening	5.6	5.2	4.6	2.6	3.0
attenuated	35.8	36.6	44.8	54.0	45.3
dynamicity (μm/min)	2.35	1.9	1.3	0.9	1.0

[a] [Tubulin] = 20 μM. Data are mean ± SD. * $P = 0.001$, except for growing and shortening lengths which are mean ± SEM. The values in the parentheses are the number of events. Control data are the same as those shown in Table 1, reproduced here for the convenience of the reader.

shortening as efficiently as the mixture of full length EB1 and p150n (Table 4, Figure 3A). Only 0.17 μM EB1-ΔC dimers, which corresponds to a 1:120 molar ratio of EB1-ΔC to tubulin, decreased the shortening rate and length shortened by 35% and 40%, respectively (Figure 3B). It also significantly reduced the catastrophe frequency (Figure 3B). A concentration of 0.25 μM EB1-ΔC, corresponding to a still low EB1-ΔC to tubulin molar ratio of 1:80, was sufficient to suppress the shortening rate and extent by 60% and 50%, respectively, and the catastrophe frequency by ~70%. Similar to EB1−p150n, EB1-ΔC also increased the growing length and the rescue frequency but did so to a lesser extent than EB1−p150n (Tables 3 and 4). Thus, similar to the effects of EB1−p150n, deletion of the C-terminus of EB1 significantly increases its ability to suppress plus end dynamics.

Binding of EB1, EB1-ΔC, and EB1−p150n to Microtubules. The relatively powerful abilities of EB1-ΔC and of the mixture of full length EB1 and p150n to suppress plus end dynamics as compared with full length EB1 alone indicate that the C-terminus of EB1 might control its ability to bind to microtubules. To test this possibility, we determined the amounts of EB1-ΔC, EB1−p150n, and full length EB1 that became bound to the microtubules at a 3.4 μM concentration of each protein (1:6 molar ratio of EB1 to tubulin) after copolymerizing tubulin and the proteins and sedimenting the microtubules through sucrose cushions to remove any unbound protein (*27*). While such an approach with single concentrations of EB1-ΔC, EB1−p150n, and full length EB1 are not as complete as they would be by use of multiple concentrations and a Scatchard analysis, the stoichiometries obtained do provide an indication of the extent to which the proteins bind to the microtubules at these relatively high EB1 concentrations. An appreciable amount of EB1 became bound to the microtubules as shown in Figure 4A, lane 1, 3. Quantitation by SDS−PAGE and densitometry (*27*) revealed that 1 mol of full length EB1 dimer bound per ~12.6 ± 1.1 mol of tubulin dimers in the microtubules, similar to the stoichiometry reported in (*14*). In three independent experiments, 1.1 μM, 0.9 μM, and 0.9 μM EB1 dimer were bound to 14.8 μM, 11.5 μM, and 10.0 μM tubulin, respectively, in the microtubules. The same concentration of EB1-ΔC bound to the microtubules at ~double the stoichiometry of EB1 dimer. Specifically, 1 mol of EB1-ΔC dimer bound ~6 ± 0.9 mol of tubulin in the microtubules (Figure 4A, lane 3). In three independent experiments, 2.7 μM, 1.8 μM, and 2.7 μM EB1-ΔC dimer were bound to 15.6 μM, 14.3 μM, and 16.6 μM tubulin, respectively, in microtubules. Like EB1-ΔC, full length EB1 when added together with p150n also bound to the microtubules with ~double the stoichiometry of full length EB1 alone. With the EB1−p150n mixture, 1 mol of EB1 became bound per ~6.6 ± 0.3 mol of tubulin dimers in the microtubules (Figure 4B, lane 2). In three independent experiments, 2.4 μM, 1.3 μM, and 2.1 μM EB1 dimer were bound to 16.6 μM, 8.6 μM, and 13.4 μM tubulin, respectively, in microtubules. Thus, the binding of C-terminal-truncated EB1 or of EB1−p150n to microtubules is significantly stronger than that of full length EB1 by itself. In addition, the presence of the C-terminus reduces the binding of EB1 to microtubules and

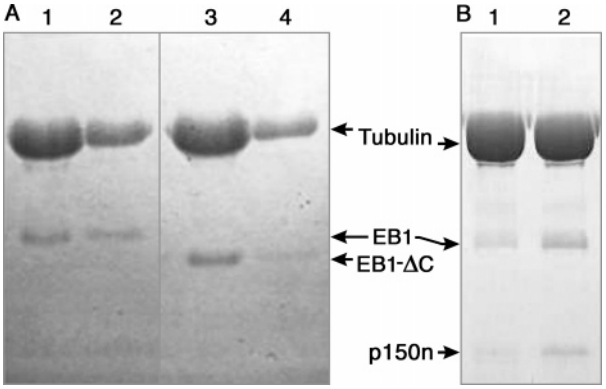

FIGURE 4: A. Binding of EB1 and EB1-ΔC to microtubules. EB1 (3.4 μM) or EB1-ΔC were copolymerized with 20 μM tubulin and the microtubules were analyzed by SDS−PAGE after centrifugation through 30% sucrose cushion (Materials and Methods). Lane 1, pellet of EB1 bound microtubules; lane 2, supernatant of unpolymerized tubulin and EB1; lane 3, pellet of EB1-ΔC bound microtubules; lane 4, supernatant of unpolymerized tubulin and EB1-ΔC. B. Binding of EB1 and EB1−p150n to microtubules. EB1 (3.4 μM) or EB1−p150n (3.4 μM) were copolymerized with 20 μM tubulin, and the microtubules were sedimented through 30% sucrose cushions and analyzed as in A. Lane 1, pellet of EB1 bound microtubules; lane 2, pellet of EB1−p150n bound microtubules. The gel images shown in A and B represent one of three independent experiments.

a significantly higher amount of EB1 is recruited to microtubules when the C-terminus is deleted or when EB1 is complexed with p150n.

DISCUSSION

We have analyzed the effects of EB1 and p150n, the N-terminal CAP-Gly domain of its +TIP binding partner $p150^{Glued}$, both individually and together as a complex, on dynamic instability at plus ends of microtubules at steady state *in vitro*. EB1 by itself suppressed plus end dynamics predominantly by strongly reducing the rate and moderately reducing the extent of shortening and moderately suppressing the catastrophe frequency (Table 1, Figure 1A, B). By itself, p150n had little effect on these parameters at a concentration as high as 2 μM (a ratio of p150n to tubulin of 1:10). However, when added together with p150n, the potency of EB1 to suppress shortening dynamics increased 3−4-fold (Table 3, Figure 2A, B). In contrast, the EB1−p150n complex significantly increases the plus end growth length and the rescue frequency. Specifically, only a 1:80 molar ratio of EB1−p150n to tubulin increased the growth length ∼1.8-fold and the rescue frequency ∼1.7-fold. After deleting the C-terminal 20 amino acid residues of EB1, which is a crucial region for p150n binding (*20*, *21*), EB1 was as effective at suppressing the rate and extent of shortening and the catastrophe frequency as was the full length EB1−p150n mixture. This indicates that in the absence of other binding partners, the flexible C-terminal tail of EB1 weakens the ability of EB1 to suppress shortening dynamics.

How Might EB1 by Itself Suppress Plus End Shortening without Affecting Growth? Previous work (*14*, *29*) and our own unpublished data have shown that EB1 does not bind to soluble tubulin. It has been shown previously in *Xenopus* extracts that EB1 binds both to the tips of microtubules and to the walls (*14*). When studied with purified microtubules, EB1 clearly binds to microtubules along their lengths (*14*). One mole of EB1 bound to ∼10−12 mol of tubulin in microtubules stabilized by paclitaxel with a moderately strong K_D of ∼0.5 μM (*14*). Along the same lines, Sandblad et al. (*30*) have also studied the binding to microtubules *in vitro* of Mal3p, the fission yeast homologue of human EB1, and have shown by cryo-electron microscopy that it binds to microtubules along the seam in the microtubule lattice.

In the present work we found that when copolymerized by itself with microtubules at a relatively high concentration of EB1 (3.4 μM) and an EB1 dimer to total tubulin ratio of 1: 6 (20 μM tubulin), 1 mol of EB1 dimer bound per ∼12 mol of tubulin dimer in the microtubules (Figure 4). This stoichiometry of EB1 binding to microtubules is reasonably close to the values reported by Tirnauer et al. (*14*) and Sandblad et al. (*30*), and further demonstrates that EB1 can bind along the microtubule lattice. The ∼1:12 molar ratio of EB1 binding to tubulin in the microtubules (i.e., ∼1 molecule of EB1 per 13 molecules of tubulin) is in agreement with the studies of Sandblad et al. (*30*), demonstrating that EB1 binds along the seam of the microtubule lattice. Notably, relatively small amounts of microtubule-bound EB1 were sufficient to reduce the rate and extent of shortening. Specifically, 30% suppression of shortening occurred at a ratio of 1 mol of EB1 dimer per 40 mol of total tubulin in the system. Thus a microtubule 10 μm in length and consisting of ∼18,900 molecules of tubulin would have no more than 460 molecules of EB1 dimer bound to it, or 1 molecule of EB1 per ∼40 molecules of tubulin. While we cannot exclude the possibility that the effects of EB1 on shortening dynamics *in vitro* are due to its binding to microtubule tips, the data are most consistent with the possibility that these effects are due to its binding along the length of the microtubules. Such a mechanism is similar to the mechanism of action of the antimitotic drug paclitaxel which, like EB1, does not bind to soluble tubulin but binds to purified microtubules along their lengths (*31*). Very little microtubule bound paclitaxel is sufficient to cause strong suppression of dynamics. Specifically, ∼1 molecule of paclitaxel bound per every 100−200 molecules of tubulin along the microtubule wall suppresses the rate and extent of shortening by 50% (*31*). Consistent with the hypothesis that EB1 alone reduces shortening dynamics by binding along microtubule surfaces, EB1 by itself reduced the catastrophe frequency only minimally and, like paclitaxel, did not exert any effects on the rate and extent of growth. Most drugs that act at the microtubule ends such as the *Vinca* alkaloids reduce the rate and extent of growth (*32*). Thus we suggest that one function of EB1 by itself in cells may be to suppress the rate and extent of microtubule shortening by binding along the lengths of microtubules.

Role of the C-Terminal Tail in Controlling EB1's Activity. Deletion of the C-terminus of EB1 increased its ability to suppress the rate and extent of shortening ∼4-fold (Table 4). However, unlike full length EB1 by itself, EB1-ΔC at a ratio as low as 1 mol of EB1-ΔC to 80 mol of tubulin exerted additional actions by significantly reducing the plus end catastrophe frequency, increasing the rescue frequency, and increasing the growth length (Table 4). We suggest that these additional effects of EB1-ΔC might best be explained by its stronger binding to microtubules than full length EB1. Further, it is reasonable to think that the effects of EB1-ΔC on the catastrophe and rescue frequencies are brought about

by the action of EB1-ΔC directly at the tips. Thus, in contrast to the mechanism of action of full length EB1, EB1-ΔC at low concentrations may modulate dynamics directly at microtubule tips.

EB1 forms a moderately stable complex with $p150^{Glued}$ by binding to its C-terminal tail (*20*, *23*). However, the functional significance of the binding is not well understood. Data obtained in migrating fibroblasts have shown that EB1 and $p150^{Glued}$ colocalize at plus ends of microtubules (*17*). It has also been reported that EB1 is required for localization of $p150^{Glued}$ at growing plus ends (*33*). It is possible that in cells an interaction between EB1 and $p150^{Glued}$ is required for their regulation of microtubule plus end dynamics. Consistent with this hypothesis, when EB1 was added together with p150n in the present study, 3−4-fold lower ratios of EB1−p150n to tubulin than EB1 itself were able to suppress the rate and extent of shortening. While p150n itself can increase the growth length and rescue frequency at plus ends, the two proteins together significantly increased these parameters at much lower concentrations than p150n alone. Also, low concentrations of EB1−p150n reduced the catastrophe frequency, an effect that might be expected to be due to a direct action at the microtubule ends.

In the presence of a relatively high molar ratio of EB1−p150n to tubulin, we found that EB1 bound to purified microtubules with higher molar stoichiometry than when EB1 was present by itself. At a 1:6 molar ratio of EB1−p150n to tubulin, there was ∼1 mol of EB1 bound to ∼6.6 mol of tubulin in the microtubules, which is double the stoichiometry of EB1 binding by itself (Figure 4). This finding suggests that p150n activated the autoinhibited state of EB1 by effectively removing the tail that prevents the most efficient binding thus enabling EB1 to bind to more tubulin subunits in the microtubule lattice than when EB1 is present by itself. Removal of the autoinhibitory C-terminal region or its binding with p150n significantly increased the efficiency of EB1 to decrease the catastrophe frequency and increase the rescue frequency. Our results demonstrating that the combination of EB1 and p150n possesses anticatastrophe activity also complement those of Tirnauer et al. (*14*) in *Xenopus* extracts which showed that added EB1 exerted anticatastrophe activity. The results also indicate that the anticatastrophe activity of EB1 in the extracts observed by Tirnauer et al. (*14*) was likely due to its action in combination with other binding partners.

In conclusion, our results strongly support the hypothesis that EB1 by itself possesses autoinhibitory activity that is regulated by its flexible C-terminal tail, and that by binding to the C-terminus, $p150^{Glued}$ abolishes the autoinhibition (*21*). Our results also suggest that in cells EB1 and $p150^{Glued}$, which colocalize at microtubule tips and presumably are both components of a dynamic +TIP protein network, might function together to regulate plus end dynamics differently than the way each protein functions on its own.

ACKNOWLEDGMENT

We thank Mr. Herbert P. Miller for preparation of purified tubulin.

REFERENCES

1. Deasi, A., and Mitchison, T. J. (1997) Microtubule polymerization dynamics, *Annu. Rev. Cell Biol. 13*, 83−117.
2. Waterman-Storer, C. M., and Salmon, E. D. (1999) Positive feedback interactions between microtubule and actin dynamics during cell motility, *Curr. Opin. Cell Biol. 11*, 61−67.
3. Wittmann, T., and Waterman-Storer, C. M. (2005) Spatial regulation of CLASP affinity for microtubules by Rac1 and GSK3beta in migrating epithelial cells, *J. Cell Biol. 169*, 929−939.
4. Panda, D., Samuel, J. C., Massie, M., Feinstein, S. C., and Wilson, L. (2003) Differential regulation of microtubule dynamics by three- and four- repeat tau: implication for the onset of neurodegenerative disease, *Proc. Natl. Acad. Sci. U.S.A. 100*, 9548−9553.
5. Rogers, G. C., Rogers, S. L., Schwimmer, T. A., Ems-McClung, S. C., Walczak, C. E., Vale, R. D., Scholey, J. M., and Sharp, D. J. (2004) Two mitotic kinesins cooperate to drive sister chromatid separation during anaphase, *Nature 427*, 364−370.
6. Schuyler, S. C., and Pellman, D. (2001) Microtubule "plus end tracking proteins": The end is just the beginning, *Cell 105*, 421−424.
7. Gundersen, G. G. (2002) Evolutionary conservation of microtubule-capture mechanisms, *Nat. Rev. Mol. Cell Biol. 3*, 296−304.
8. Howard, J., and Hyman, A. A. (2003) Dynamics and mechanics of the microtubule plus end, *Nature 422*, 753−758.
9. Galjart, N., and Perez, F. (2003) A plus-end raft to control microtubule dynamics and function, *Curr. Opin. Cell Biol. 15*, 48−53.
10. Carvalho, P., Tirnauer, J. S., and Pellman, D. (2003) Surfing on microtubule ends, *Trends Cell Biol. 13*, 229−237.
11. Vaughan, K. T. (2004) Surfing, regulating and capturing: are all microtubule-tip-tracking proteins created equal, *Trends Cell Biol. 14*, 491−496.
12. Akhmanova, A., and Hoogenrad, C. C. (2005) Microtubule plus-end-tracking proteins: mechanisms and functions, *Curr. Opin. Cell Biol. 17*, 47−54.
13. Morrison, E. E. (2007) Action and interactions at microtubule ends, *Cell Mol. Life Sci. 64*, 307−317.
14. Tirnauer, J. S., Grego, S., Salmon, E. D., and Mitchison, T. J. (2002) EB1-microtubule interactions in Xenopus egg extracts: role of EB1 in microtubule stabilization and mechanisms of targeting to microtubules, *Mol. Biol. Cell 13*, 3614−3626.
15. Schroer, T. A. (2004) Dynactin, *Annu. Rev. Cell Dev. Biol. 20*, 759−779.
16. Vaughan, K. T., Tynan, S. H., Faulkner, N. E., Echeverri, C. J., and Vallee, R. B. (1999) Colocalization of cytoplasmic dynein with dynactin and CLIP 170 at microtubule distal ends, *J. Cell Sci. 112*, 1437−1447.
17. Ligon, L. A., Shelly, S. S., Tokito, M., and Holzbour, E. L. F. (2003) The microtubule plus end proteins EB1 and dynactin have differential effects on microtubule polymerization, *Mol. Biol. Cell 14*, 1405−1417.
18. Culver-Hanlon, T. L., Lex, S. A., Stephens, A. D., Quintyne, N. J., and King, S. J. (2006) A microtubule-binding domain in dynactin increases dynein processivity by skating along microtubules, *Nat. Cell Biol. 8*, 264−270.
19. Kim, H., Ling, S. C., Rogers, G. C., Kural, C., Selvin, P. R., Rogers, S. L., and Gelfand, V. I. (2007) Microtubule binding by dynactin is required for microtubule organization but not cargo transport, *J. Cell Biol. 176*, 641−651.
20. Honnappa, S., Okhrimenko, O., Jaussi, R., Jawhari, H., Jelesarov, I., Winkler, F. K., and Steinmetz, M. O. (2006) Key interaction modes of dynamic +TIP networks, *Mol. Cell 23*, 663−671.
21. Hayashi, I., Wilde, A., Mal, T. K., and Ikura, M. (2005) Structural basis for the activation of microtubule assembly by the EB1 and p150Glued complex, *Mol. Cell 19*, 449−460.
22. Honnappa, S., John, C. M., Kostrewa, D., Winkler, F. K., and Steinmetz, M. O. (2005) Structural insights into the EB1-APC interaction, *EMBO J. 24*, 261−269.
23. Weisbrich, A., Honnappa, S., Jaussi, R., Okhrimenko, O., Frey, D., Jelesarov, I., Akhmanova, A., and Steinmetz, M. O. (2007) Structure-function relationship of CAP-Gly domains, *Nat. Struct. Mol. Biol. 14*, 959−967.
24. Panda, D., Jordan, M. A., Chu, K. C., and Wilson, L. (1996) Differential effects of vinblastine on microtubule polymerization and dynamics at opposite microtubule ends, *J. Biol. Chem. 271*, 29807−29812.
25. Bradford, M. M. (1976) A rapid and sensitive method for the quantitation of microgram quantities of protein utilizing the principle of protein-dye binding, *Anal. Biochem. 72*, 248−254.

26. Manna, T., Thrower, D. A., Miller, H. P., Curmi, P., and Wilson, L. (2006) Stathmin strongly increases the minus end catastrophe frequency and induces rapid treadmilling of bovine brain microtubules, *J. Biol. Chem. 281*, 2071−2078.
27. Manna, T., Grenningloh, G., Miller, H. P., and Wilson, L. (2007) Stathmin family protein SCG10 differentially regulates the plus and minus end dynamics of microtubules at steady state in vitro: implications for its role in neurite outgrowth, *Biochemistry 46*, 3543−3552.
28. Berrueta, L., Tirnauer, J. S., Schuyler, S. C., Chen, L. B., Hill, D. E., Pellman, D., and Bierer, B. E. (1999) The APC-associated protein EB1 associates with components of the dynactin complex and cytoplasmic dynein intermediate chain, *Curr. Biol. 9*, 425−428.
29. Niethammer, P., Kronja, I., Kandels-Lewis, S., Rybina, S., Bastiaens, P., and Karsenti, E. (2007) Discrete states of a protein interaction network govern interphase and mitotic microtubule dynamics, *PLoS Biol. 5*, e29.
30. Sandblad, L., Busch, K. E., Tittmann, P., Gross, H., Brunner, D., and Hoenger, A. (2006) The Schizosaccharomyces probe EB1 homolog Mal3p binds and stabilizes the microtubule lattice seam, *Cell 127*, 1415−1424.
31. Derry, W. B., Wilson, L., and Jordan, M. A. (1995) Substoichiometric binding of Taxol suppresses microtubule dynamics, *Biochemistry 34*, 2203−2211.
32. Jordan, M. A., and Wilson, L. (2004) Microtubules as a target for anticancer drugs, *Nat. Rev. Cancer 4*, 253−265.
33. Watson, P., and Stephens, D. J. (2006) Microtubule plus end loading of p150(Glued) is mediated by EB1 and CLIP-170 but is not required for intracellular membrane traffic in mammalian cells, *J. Cell Sci. 119*, 2758−2767.
34. Bu, W., and Su, L. K. (2001) Regulation of microtubule assembly by human EB1 family proteins, *Oncogene 20*, 3185−3192.
35. Waterman-Storer, C. M., Karki, S., and Holzbaur, E. L. (1995) The p150Glued component of the dynactin complex binds to both microtubules and the actin related protein centractin (Arp-1), *Proc. Natl. Sci. Acad. U.S.A. 92*, 1634−1638.

BI701912G